

# Sunyaev – Zel’dovich fluctuations from spatial correlations between clusters of galaxies

Eiichiro Komatsu

Astronomical Institute, Tôhoku University,  
Aoba, Sendai 980-8578, Japan

Tetsu Kitayama

Theoretical Astrophysics Group, Department of Physics, Tokyo Metropolitan University,  
Hachioji, Tokyo 192-0397, Japan

## ABSTRACT

We present angular power spectra of the cosmic microwave background radiation anisotropy due to fluctuations of the Sunyaev-Zel’dovich (SZ) effect through clusters of galaxies. A contribution from the correlation among clusters is especially focused on, which has been neglected in the previous analyses. Employing the evolving linear bias factor based on the Press-Schechter formalism, we find that the clustering contribution amounts to 20 – 30% of the Poissonian one at degree angular scales. If we exclude clusters in the local universe, it even exceeds the Poissonian noise, and makes dominant contribution to the angular power spectrum. As a concrete example, we demonstrate the subtraction of the *ROSAT* X-ray flux-limited cluster samples. It indicates that we should include the clustering effect in the analysis of the SZ fluctuations. We further find that the degree scale spectra essentially depend upon the normalization of the density fluctuations, i.e.,  $\sigma_8$ , and the gas mass fraction of the cluster, rather than the density parameter of the universe and details of cluster evolution models. Our results show that the SZ fluctuations at the degree scale will provide a possible measure of  $\sigma_8$ , while the arc-minute spectra a probe of the cluster evolution. In addition, the clustering spectrum will give us valuable information on the bias at high redshift, if we can detect it by removing X-ray luminous clusters.

*Subject headings:* cosmology: cosmic microwave background – galaxies: clusters

## 1. Introduction

The cosmic microwave background radiation (CMBR) anisotropy is now known as the most powerful probe of our Universe (e.g. Hu, Sugiyama & Silk 1997). In addition to the *primary* anisotropy which will give us clues to most of the cosmological parameters within 10% accuracy (Bond, Efstathiou & Tegmark 1997), there is the *secondary* anisotropy caused by several processes in the low-redshift universe, e.g., non-linear evolution of gravitational structures (Rees & Sciama 1968), peculiar velocity field of re-ionized clumps (Ostriker & Vishniac 1987), and the Sunyaev-Zel’dovich (SZ) effect through clusters of galaxies. The SZ effect is the brightness change of the CMBR due to inverse Compton scattering by hot electrons (Zel’dovich & Sunyaev 1969; Sunyaev & Zel’dovich 1972). So far the brightness *decrement* in the Rayleigh-Jeans band

has been detected toward tens of clusters (see, Birkinshaw 1999 for review), and we have recently detected the *increment* in the Wien band (Komatsu et al. 1999). Thanks to such specific spectral features, one will be able to separate the SZ fluctuations (SZF) rather accurately from any other signals using future satellite observations, e.g., that of *PLANCK* surveyor (Hobson et al. 1998). Furthermore, the SZF should provide a probe of high- $z$  clusters yet to be detected otherwise, because the SZ brightness is free from the redshift diminishing effect (Birkinshaw 1999) unlike the X-ray brightness.

Although several theoretical studies have been done on the SZF (Rephaeli 1981; Ostriker & Vishniac 1986; Cole & Kaiser 1988; Schaeffer & Silk 1988; Markevitch et al. 1991; Makino & Suto 1993; Bartlett & Silk 1994; Persi et al. 1995; Bond & Myers 1996; Atrio-Barandera & Mucket 1999), they mainly focus on the Poissonian component only and much less attention is paid to that arisen from the cluster-cluster correlation. In this Letter, we point out that the cluster-cluster correlation can in fact make a non-negligible contribution to the SZF at degree scales and explicitly predict its angular power spectra. We further investigate possibilities of exploring the nature of density fluctuations, cluster gas distributions, and clustering properties of high-redshift clusters, by means of the SZF.

## 2. Model

### 2.1. Angular Profile of a Cluster

The gas density profile of each cluster is approximated by the spherical isothermal  $\beta$ -model,  $\rho_{\text{gas}}(r) = \rho_{\text{gas}0} \left[1 + (r/r_c)^2\right]^{-3\beta/2}$ , where  $r_c$  is the core radius, and  $\rho_{\text{gas}0}$  is the central gas mass density. To account for the fact that a real cluster has a finite size, we introduce the Gaussian filter on the edge at radius  $R$ , i.e.,  $\rho_{\text{gas}}(r) \rightarrow \rho_{\text{gas}}(r)e^{-r^2/\xi R^2}$ , where  $\xi$  is a fudge factor to normalize the total gas mass of a cluster. Assuming  $\beta = 2/3$  for simplicity, the gas mass contained within  $R$  is

$$M_{\text{gas}} \equiv \int_0^R dV \rho_{\text{gas}}(r) = 4\pi \rho_{\text{gas}0} r_c^3 (p - \arctan p), \quad (1)$$

where  $p \equiv R/r_c$ . On the other hand,

$$\int_0^\infty dV \rho_{\text{gas}}(r) e^{-r^2/\xi R^2} = 4\pi \rho_{\text{gas}0} r_c^3 h(p), \quad (2)$$

where

$$h(p) \equiv p \sqrt{\frac{\pi}{4} \xi} - \frac{\pi}{2} e^{1/\xi p^2} \text{Erfc} \left( \sqrt{1/\xi p^2} \right), \quad (3)$$

and  $\text{Erfc}(u)$  is the complementary error function. Matching equations (1) and (2) at  $p \gg 1$  gives  $\xi = 4/\pi$ .

The above density profile yields the angular temperature profile projected on the sky due to the SZ effect in terms of the ‘‘Compton  $y$ -parameter’’ (Zel’dovich & Sunyaev 1969) as

$$\frac{\Delta T(\theta)}{T_{\text{cmb}}} = g(x)y(\theta), \quad (4)$$

$$y(\theta) = \sigma_T n_{e0} r_c \left( \frac{k_B T_e}{m_e c^2} \right) \times \frac{\pi e^{1/\xi p^2}}{\sqrt{1 + (\theta/\theta_c)^2}} \text{Erfc} \left( \sqrt{\frac{1 + (\theta/\theta_c)^2}{\xi p^2}} \right), \quad (5)$$

where  $T_{\text{cmb}} = 2.728\text{K}$  (Fixsen et al. 1996),  $g(x) \equiv x \coth(x/2) - 4$ ,  $x \equiv h\nu/k_B T_{\text{cmb}}$ ,  $n_{e0}$  is the central electron number density,  $T_e$  is the electron temperature, and other physical constants have their usual

meanings. The angular core size  $\theta_c$  is related to  $r_c$  via  $\theta_c = r_c/d_A(z)$ , where  $d_A$  is the angular diameter distance to a cluster at redshift  $z$ .

We model that clusters have virialized at  $z$  and relate the quantities  $R$ ,  $T_e$ ,  $n_{e0}$  and  $r_c$  to the total mass  $M$  and redshift  $z$  based on the spherical infall model (Peebles 1980, §19). We assume that  $R$  is equal to the virial radius,  $R = [3M/4\pi\rho_{\text{univ}}(z)\Delta_c(z)]^{1/3}$ , where  $\rho_{\text{univ}}(z)$  is the mean density of the universe, and  $\Delta_c(z)$  is the mean density of a cluster in units of  $\rho_{\text{univ}}(z)$  given in Lacey & Cole (1993) and Nakamura & Suto (1997) for an arbitrary cosmology. Then the electron temperature is expressed as  $k_B T_e = \eta\mu m_p GM/3R$ , using the mean molecular weight  $\mu$  and a fudge factor of order unity  $\eta$ , for which we adopt  $\mu = 0.59$  and  $\eta = \beta^{-1} = 3/2$ , respectively. The central electron number density is derived with the help of equation (2) as  $n_{e0} = (\rho_{\text{gas0}}/m_p)(X+1)/2 = (Mf_{\text{gas}}/m_p 4\pi r_c^3 h(p))(X+1)/2$ , where we fix the hydrogen abundance at  $X = 0.76$  and assume that the gas mass fraction is equal to the cosmological mean,  $f_{\text{gas}} = M_{\text{gas}}/M = \Omega_b/\Omega_0$  (White et al. 1993). Given large uncertainties in the formation of cluster core regions, we analyze two different scenarios for the evolution of  $r_c$ , i.e., the *self-similar* (SS) model (Kaiser 1986), and the *entropy-driven* (ED) model (Kaiser 1991; Evrard & Henry 1991; Bower 1997). In the SS model,  $r_c$  is simply proportional to the virial radius,

$$p_{\text{ss}}(M, z) = \text{constant}. \quad (6)$$

In the ED model, on the other hand, the core is in a minimum entropy phase,  $s_{\text{min}} = c_V \ln(T_e/\rho_{\text{gas0}}^{\gamma-1})$ , and its evolution is specified by  $s_{\text{min}}(z) = s_{\text{min}}(z=0) + c_V \epsilon \ln(1+z)$  with a free parameter  $\epsilon$ , yielding

$$\begin{aligned} p_{\text{ed}}(M, z) &\approx \left( \frac{3\rho_{\text{gas0}}(M, z)/f_{\text{gas}}}{\rho_{\text{univ}}(z)\Delta_c(z)} \right)^{1/2} \\ &\propto \frac{T_e^{\frac{1}{2(\gamma-1)}}(M, z)}{\Delta_c^{1/2}(z)} (1+z)^{-\frac{3}{2} - \frac{\epsilon}{2(\gamma-1)}}, \end{aligned} \quad (7)$$

where we have used  $M = (4\pi/3)\rho_{\text{univ}}(z)\Delta_c(z)R^3 \approx 4\pi(\rho_{\text{gas0}}/f_{\text{gas}})r_c^3 p$  for  $p \gg 1$ . The adiabatic index is fixed at  $\gamma = 5/3$  throughout. Since Mushotzky & Scharf (1997) obtained the constraint of  $\epsilon = 0 \pm 0.9$  from X-ray cluster samples, we demonstrate three cases of  $\epsilon = -1, 0, 1$  in the same way as Atrio-Barandela & Mücke (1999). We normalize the proportional constants in both models at  $M = 10^{15} h^{-1} M_\odot$  and  $z = 0$  assuming  $r_c(10^{15} h^{-1} M_\odot, z = 0) = 0.15 h^{-1} \text{Mpc}$ .

## 2.2. Angular Power Spectrum

One conventionally expands the angular two-point correlation function of the temperature distribution in the sky into the Legendre Polynomial:

$$\left\langle \frac{\Delta T}{T_{\text{cmb}}}(\mathbf{n}) \frac{\Delta T}{T_{\text{cmb}}}(\mathbf{n} + \boldsymbol{\theta}) \right\rangle = \frac{1}{4\pi} \sum_l C_l P_l(\cos \theta). \quad (8)$$

Since we are considering discrete sources, we can write  $C_l = C_l^{(P)} + C_l^{(C)}$ , where  $C_l^{(P)}$  is the contribution from the Poissonian noise and  $C_l^{(C)}$  is from the correlation among clusters (Peebles 1980, §41). For convenience, we define the power spectrum of  $y$ -parameter,  $C_l^{yy} \equiv C_l/g^2(x)$ , which is independent of frequency. Following Cole & Kaiser (1988) and employing Limber's equation in the cosmological context (e.g., Peebles 1980, §56), we get an integral expression of  $C_l^{yy(P,C)}$ :

$$C_l^{yy(P)} = \int_0^{z_{\text{dec}}} dz \frac{dV}{dz} \int_{M_{\text{min}}}^{M_{\text{max}}} dM \frac{dn(M, z)}{dM} |y_l(M, z)|^2, \quad (9)$$

$$C_l^{yy(C)} = \int_0^{z_{\text{dec}}} dz \frac{dV}{dz} P_m \left( k = \frac{l}{r(z)}, z \right) \left[ \int_{M_{\text{min}}}^{M_{\text{max}}} dM \Phi_l(M, z) \right]^2, \quad (10)$$

where  $V(z)$  and  $r(z)$  are the comoving volume and the comoving distance, respectively,  $\Phi_l(M, z)$  is the “biased temperature function”:

$$\Phi_l(M, z) \equiv \frac{dn(M, z)}{dM} b(M, z) y_l(M, z), \quad (11)$$

and  $y_l$  is the angular Fourier transform of  $y(\theta)$ . In equations (9) and (10),  $z_{\text{dec}}$  is the redshift of photon decoupling, and we choose  $M_{\text{min}} = 5 \times 10^{13} h^{-1} M_{\odot}$  and  $M_{\text{max}} = 5 \times 10^{15} h^{-1} M_{\odot}$  to bracket the mass scale of clusters. The mass function  $dn/dM$  is computed using the Press-Schechter formula (Press & Schechter 1974):

$$\frac{dn(M, z)}{dM} = \sqrt{\frac{\pi}{2}} \frac{\rho_{\text{univ}}(0)}{M} \left| \frac{d \ln \sigma(M)}{dM} \right| \nu(M, z) e^{-\nu^2(M, z)/2}, \quad (12)$$

where  $\sigma(M)$  is the present-day rms mass fluctuation within the top-hat filter,  $\nu(M, z) \equiv \delta_c(z)/D(z)\sigma(M)$  is the “peak-height threshold”,  $D(z)$  is the linear growth factor of density fluctuations, and  $\delta_c(z)$  is the threshold overdensity of spherical collapse given in Lacey & Cole (1993) and Nakamura & Suto (1997) for an arbitrary cosmological model. We assume that the matter power spectrum,  $P_m(k, z)$ , is related to the power spectrum of the cluster correlation function,  $P_c(k, M_1, M_2, z)$ , via the time-dependent linear bias factor,  $b(M, z)$ , i.e.,  $P_c(k, M_1, M_2, z) = b(M_1, z)b(M_2, z)D^2(z)P_m(k, z=0)$ . We adopt for  $b(M, z)$  an analytic formula derived by Mo & White (1996):  $b(M, z) = 1 + (\nu^2(M, z) - 1)/\delta_c(z)$ , which shows an excellent agreement with numerical simulations at the cluster mass scale (Jing 1998, 1999). To calculate  $P_m(k)$ , we employ the Harrison-Zel’dovich spectrum and the transfer function of Bardeen et al. (1986) with the shape parameter given in Sugiyama (1995). Unless stated explicitly, we assume the  $\Lambda$ CDM cosmology with  $\Omega_0 = 0.3$ ,  $\lambda_0 = 0.7$ ,  $\Omega_b = 0.05$ ,  $h = 0.7$  and  $\sigma_8 = 1.0$ , which agrees with both the COBE normalization and the cluster abundance (e.g. Kitayama & Suto 1997).

### 3. Results and Discussions

#### 3.1. Poissonian and Clustering Contributions to the Sunyaev-Zel’dovich Fluctuations

Figure 1 shows the predicted power spectra of  $y$ -parameter,  $C_l^{yy(P,C)}$ , in the SS and three ED ( $\epsilon = -1, 0, 1$ ) models. The correlation term  $C_l^{yy(C)}$  amounts to around one-fifth of the Poissonian term  $C_l^{yy(P)}$  at  $l \lesssim 100$ , and we will show later that  $C_l^{yy(C)}$  even dominates  $C_l^{yy(P)}$  in some practical situations (Figure 2).

For comparison, the primary anisotropy expected in units of the Rayleigh-Jeans temperature is overlaid on the same figure. The SZF signals are shown to be sub-dominant except at  $l \gtrsim 2000$ . However, the simulations of Hobson et al. (1998) indicate that the SZF can be separately reconstructed from the CMBR map by the *PLANCK* satellite with great accuracy especially at large angular scales ( $l \lesssim 500$ ). This is fully due to the specific spectral features of the SZ effect in contrast to the primary signal and other secondary sources. The angular resolution of the *PLANCK*, on the other hand, seriously limits the accuracy of reconstruction at small angular scales ( $l \gtrsim 1000$ ).

The SZF spectra at  $l \lesssim 500$  is quite insensitive to the details of core evolution models. This feature can

be understood by looking at the angular Fourier transformation of  $y(\theta)$  (see eq. [5]):

$$y_l \propto \begin{cases} n_{e0} r_c \theta_c e^{-l\theta_c} / l & (l\theta_c \gg 1), \\ n_{e0} r_c \theta_c^2 & (l\theta_c \ll 1). \end{cases} \quad (13)$$

The spectrum at large angular scales is solely determined by the gas mass:  $y_{l \ll \theta_c^{-1}} \propto M_{\text{gas}}$ , while the small scale spectrum depends on the core radius:  $y_{l \gg \theta_c^{-1}} \propto M_{\text{gas}} e^{-l\theta_c} / (lr_c)$ . In what follows, therefore, we focus mainly on the large scale spectrum and consider only the SS model.

In practical observations, one can remove from the reconstructed SZF map bright clusters already detected in X-ray observations, e.g., by *ROSAT* satellite. Figure 2 illustrates the expected SZF spectra after excluding the clusters above some threshold X-ray fluxes,  $S_X(0.5 - 2\text{keV}) = 10^{-12}$  and  $10^{-13}$  erg cm<sup>-2</sup> s<sup>-1</sup>. These values roughly correspond to the limiting fluxes in the *ROSAT* All-Sky Survey (Ebeling et al. 1997) and the *ROSAT* Deep Cluster Survey (Rosati et al. 1998). To compute the X-ray fluxes of clusters, we have used the same method as described in Kitayama & Suto (1997), assuming the following form for the  $L_X - T$  relation:

$$L_X = L_{6\text{keV}} \left( \frac{k_B T}{6 \text{ keV}} \right)^\alpha (1+z)^\zeta \text{ erg s}^{-1}, \quad (14)$$

with  $L_{6\text{keV}} = 2.9 \times 10^{44} h^{-2}$ ,  $\alpha = 3.4$  and  $\zeta = 0$  (David et al. 1993; Mushotzky & Scharf 1997), and the X-ray band correction according to the emission model by Masai (1984).

We find that the Poissonian term  $C_l^{yy(P)}$  is greatly reduced by the subtraction of X-ray bright clusters, and the correlation term  $C_l^{yy(C)}$  indeed dominates at  $l < 200$ . This reflects the greater contribution of the correlation term  $C_l^{yy(C)}$  at higher  $z$  and smaller  $l$ , since  $C_l^{yy(C)} / C_l^{yy(P)} \sim n(M, z) P_c(k = l/r(z)) \sim n(M, z) b^2(M, z) D^2(z) r(z) / l$ , where  $P_m(k) \sim k^{-1}$  on cluster scales. Therefore, we should take into account  $C_l^{yy(C)}$  in the analysis of the SZF, and it will possibly be detected by the *PLANCK* with removing the *ROSAT* clusters.

Now, what does  $C_{l \leq 1000}^{yy(C)}$  mean after this subtraction? It should represent the clustering properties of high- $z$  clusters currently unresolved in X-ray observations. It should be noted that the above predictions depend on the linear bias assumption and the evolution history of the bias factor. Thus, if we could measure  $C_l^{yy(C)}$  separately from  $C_l^{yy(P)}$ , it would in turn provide the information on the bias at high- $z$ .

### 3.2. Implications on Cosmology

Figure 3 further illustrates the  $\sigma_8$  dependence of  $C_{l=100}^{yy(P,C)}$  in three representative cosmological models:  $\Lambda$ CDM, SCDM ( $\Omega_0 = 1$ ,  $\lambda = 0$ ,  $h = 0.5$ ) and OCDM ( $\Omega_0 = 0.45$ ,  $\lambda = 0$ ,  $h = 0.7$ ). The SZF spectra are extremely sensitive to  $\sigma_8$  while less sensitive to  $\Omega_0$  and  $\lambda_0$ . The correlation term  $C_l^{(C)}$  is more sensitive to  $\sigma_8$  than  $C_l^{(P)}$ , and can be fitted roughly by  $C_l^{(C)} \propto \sigma_8^{1.5} C_l^{(P)}$ . Since the *PLANCK* will provide the accurate angular power spectrum of the SZF at the degree angular scales (Hobson et al. 1998), they will provide a plausible measure of  $\sigma_8$ . Furthermore, figures 1 and 3 suggest that the degree scale spectrum is free from both unknown core physics of clusters and density parameters of the universe.

Bond, Efstathiou & Tegmark (1997) found that the expected  $1\sigma$  error of  $\sigma_8$  determined by the *PLANCK* using the primary anisotropies alone is as large as 20%, which corresponds to changes in  $C_l^{(P)}$  by a factor of 3 and  $C_l^{(C)}$  by a factor of 4. Figure 4 shows the total (Poissonian + clustering) and Poissonian angular power spectra of the SZF in units of the Rayleigh-Jeans temperature,  $\Delta T_l \equiv T_{\text{cmbr}} \sqrt{l(l+1)C_l}$ . We show both cases of including and excluding the X-ray bright clusters with  $S_X > 10^{-13}$  erg cm<sup>-2</sup> s<sup>-1</sup>. It

illustrates how much the SZF change within 20% error of  $\sigma_8$ . Notice that  $C_l$  without X-ray clusters has a bending structure at  $l \sim 200$ , below which  $C_l^{(C)}$  exceeds  $C_l^{(P)}$ . The spectral shape also changes with  $\sigma_8$  because  $C_l^{(P)}$  and  $C_l^{(C)}$  depend differently on  $\sigma_8$ . Such features should be quite helpful in detecting the clustering contribution separately from the Poissonian one and probing the structure formation in the high- $z$  universe. For comparison, we also plot the primary anisotropy spectrum and observational upper bounds obtained by OVRO (Readhead et al. 1989) and ATCA (Subrahmanyan et al. 1998).

The SZF should play a complementary role to the primary anisotropies in the determination of  $\sigma_8$ , and the clustering contribution hopefully brings us fruitful information of high- $z$  bias. It should be noticed, however, that these results are based upon the assumption of  $f_{\text{gas}} = \Omega_b/\Omega_0$ . We found a rough scaling relation:  $C_l^{(P)} \propto f_{\text{gas}}^2 \sigma_8^6 \Omega_0^2 h$ , at degree angular scale, and it gives  $C_l^{(P)} \propto \Omega_0^2$  when we specify  $f_{\text{gas}}$  without cosmological parameters. Uncertainties in  $f_{\text{gas}}$  yield systematic errors in the amplitude of predicted SZF angular spectrum. These points will be discussed in greater detail in future publications.

We thank Naoshi Sugiyama and Yasushi Suto for valuable suggestions, Toshifumi Futamase, Makoto Hattori, Masahiro Takada and Keiichi Umetsu for frequent discussions and critical comments. We acknowledge fellowships from Japan Society for the Promotion of Science.

## REFERENCES

- Atrio-Barandela, F., & Mücke, J. P. 1999, *ApJ*, 515, 465
- Bardeen, J. M., Bond, J. R., Kaiser, N., & Szalay, A. S. 1986, *ApJ*, 304, 15
- Bartlett, J. G., & Silk, J. 1994, *ApJ*, 423, 12
- Birkinshaw, M. 1999, *Phys. Rep.*, 310, 97
- Bond, J. R., Efstathiou, G., & Tegmark, M. 1997, *MNRAS*, 291, L33
- Bond, J. R., & Myers, S. T. 1996, *ApJS*, 103, 1
- Bower, R. G. 1997, *MNRAS*, 288, 355
- Catelan, P., Lucchin, F., Matarrese, S., & Porciani, C. 1998, *MNRAS*, 297, 692
- Cole, S., & Kaiser, N. 1988, *MNRAS*, 233, 637
- David, L. P., Slyz, A., Jones, C., Forman, W., Vrtilik, S. D., & Arnaud, K. A. 1993, *ApJ*, 412, 479
- Ebeling, H., Edge, A. C., Fabian, A. C., Allen, S. W., & Crawford C. S. 1997, *ApJ*, 479, L101
- Evrard, A. E., & Henry, J. P. 1991, *ApJ*, 383, 95
- Fixsen, D. J., Cheng, E. S., Gales, J. M. Mather, J. C., Shafer, R. A., & Wright, E. L. 1996, *ApJ*, 473, 576
- Hobson, M. P., Jones, A. W., Lasenby, A. N., & Bouchet, F. R. 1998, *MNRAS*, 300, 1
- Hu, W., Sugiyama, N., & Silk, J. 1997, *Nature*, 386, 37
- Jing, Y. P. 1998, *ApJ*, 503, L9
- Jing, Y. P. 1999, *ApJ*, 515, L1

- Kaiser, N. 1986, MNRAS, 222, 323
- Kaiser, N. 1991, ApJ, 383, 104
- Kitayama, T., & Suto, Y. 1997, ApJ, 490, 557
- Komatsu, E., Kitayama, T., Suto, Y., Hattori, M., Kawabe, R., Matsuo, H., Schindler, S., & Yoshikawa, K. 1999, ApJ, 516, L1
- Lacey, C., & Cole, S. 1993, MNRAS, 262, 627
- Makino, N., & Suto, Y. 1993, ApJ, 405, 1
- Markevitch, M., Blumenthal, G. R., Forman, W., Jones, C., & Sunyaev, R. A. 1991, ApJ, 378, L33
- Masai, K. 1984, Ap&SS, 98, 367
- Mo, H. J., & White, D. M. 1996, MNRAS, 282, 347
- Mushotzky, R. F., & Scharf, C. A. 1997, ApJ, 482, L13
- Nakamura, T. T., & Suto, Y. 1997, Prog. Theor. Phys., 97, 49
- Ostriker, J. P., & Vishniac, E. T. 1986, ApJ, 306, L51
- Peebles, P. J. E. 1980, The Large Scale Structure of the Universe (Princeton: Princeton Univ. Press)
- Persi, F. M., Spergel, D. N., Cen, R., & Ostriker, J. P. 1995, ApJ, 442, 1
- Press, W. H., & Schechter, P. 1974, ApJ, 187, 425
- Readhead, A. C. S., Lawrence, C. R., Myers, S. T., Sargent, W. L. W., Hardebeck, H. E., & Moffet, A. T. 1989, ApJ, 346, 566
- Rees, M. J., & Sciama, D. W. 1968, Nature, 517, 611
- Rosati, P., Della Ceca, R., Norman, C., & Giacconi, R. 1998, ApJ, 492, L21
- Shaeffer, R., & Silk, J. 1988, ApJ, 333, 509
- Subrahmanyam, R., Kesteven, M. J., Ekers, R. D., Sinclair, M., & Silk, J. 1998, MNRAS, 298, 1189
- Sugiyama, N. 1995, ApJS, 100, 281
- Sunyaev, R. A., & Zel'dovich, Ya. B. 1972, Comments Astrophys. Space Phys., 4, 173
- White, S. D. M., Navarro, J. F., Evrard, A. E., & Frenk, C. S. 1993, Nature, 366, 429
- Zel'dovich, Ya. B., & Sunyaev, R. A. 1969, Ap&SS, 4, 301

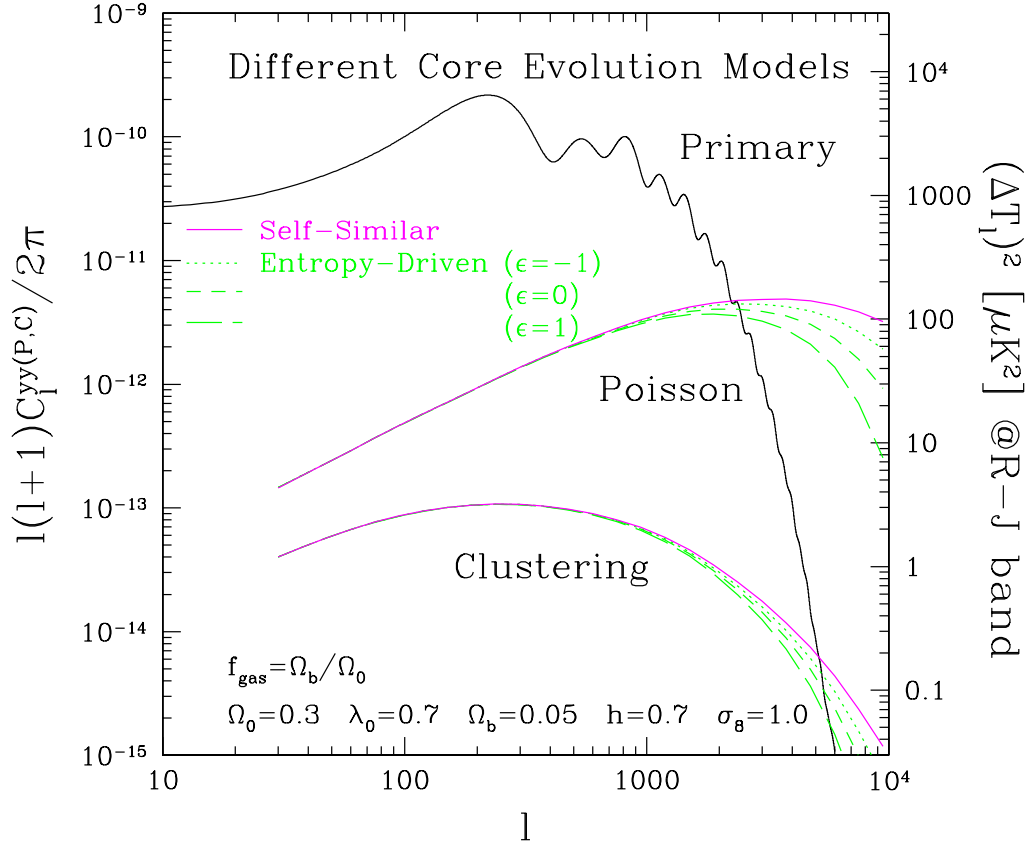


Fig. 1.— Angular power spectra of the Sunyaev-Zel’dovich fluctuations in terms of  $y$ -parameter (see text for definitions). The Poissonian and clustering spectra are shown for different core evolution models. Solid lines represent the self-similar model, while others the entropy-driven model with  $\epsilon = -1, 0, 1$  from top to bottom. Also plotted for reference is the primary temperature anisotropy expected in the Rayleigh-Jeans band (*right vertical axis*).

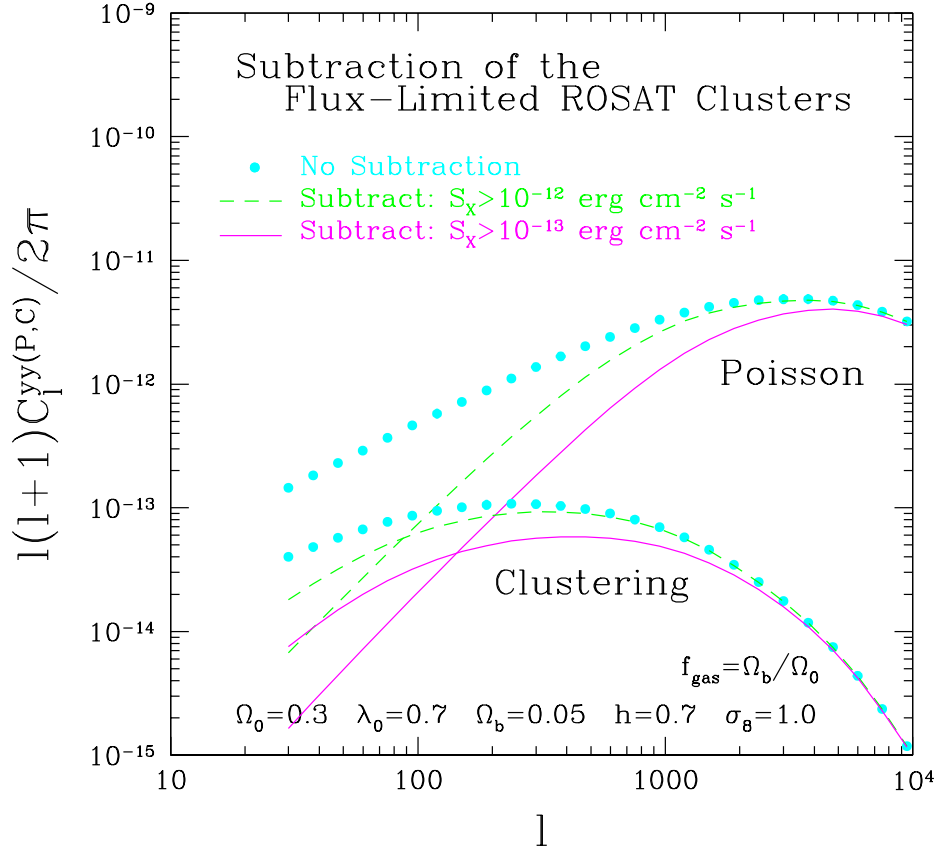


Fig. 2.— Effects of subtracting the clusters already resolved in the X-ray band. Filled circles show the angular power spectra without the subtraction. Dashed and solid lines are the spectra after removing the X-ray clusters above the flux limit of  $10^{-12}$  and  $10^{-13} \text{ erg cm}^{-2} \text{ s}^{-1}$  in the 0.5 – 2keV band, respectively.

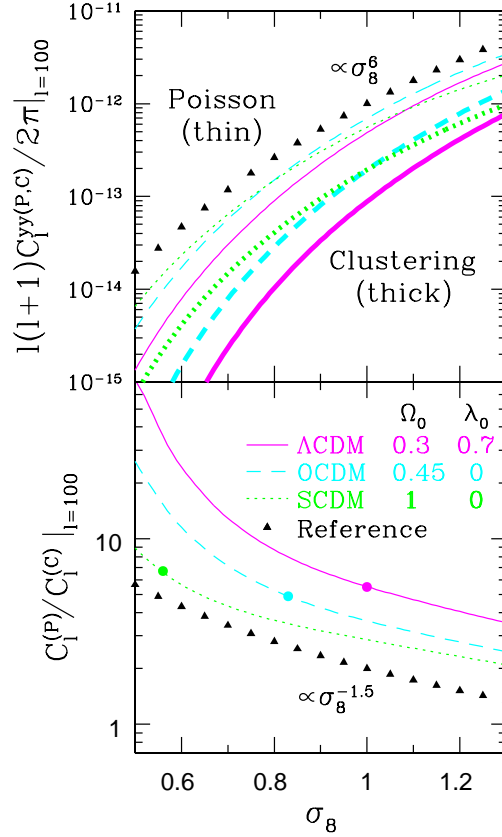


Fig. 3.— Dependences on  $\sigma_8$  of angular power spectra at  $l = 100$  in three representative cosmological models,  $\Lambda$ CDM (*solid lines*), OCDM (*dashed*) and SCDM (*dotted*). The upper panel shows the Poissonian (*thin lines*) and clustering (*thick lines*) power spectra separately, while the lower panel illustrates ratios between them. Filled triangles indicate reference lines  $\propto \sigma_8^6$  and  $\propto \sigma_8^{-1.5}$  in the upper and lower panels, respectively. Filled circles in the lower panel represent the  $\sigma_8$  value inferred from the cluster abundance in each cosmological model (Kitayama & Suto 1997).

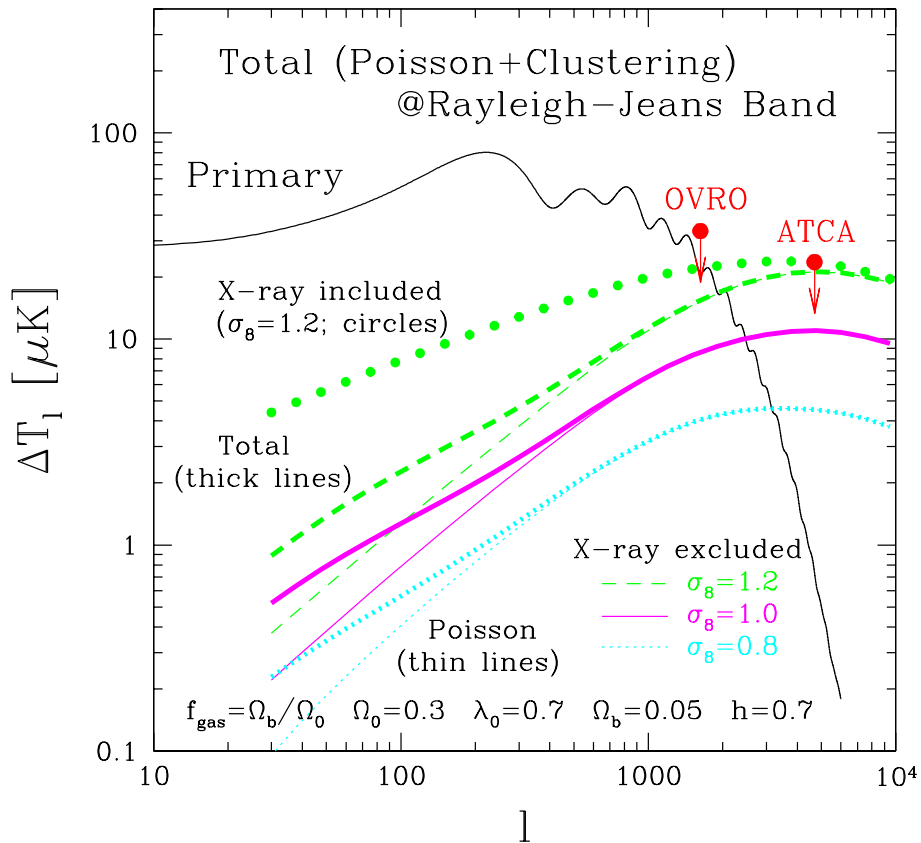


Fig. 4.— Total (*thick lines*) and Poissonian (*thin lines*) angular power spectra of the Sunyaev-Zel'dovich fluctuations in the Rayleigh-Jeans band excluding the X-ray bright clusters with  $S_X(0.5 - 2\text{keV}) > 10^{-13} \text{ erg cm}^{-2} \text{ s}^{-1}$ . Dotted, solid and dashed lines represent the cases of  $\sigma_8 = 0.8, 1.0$  and  $1.2$ , respectively. Circles show the total power spectrum with the X-ray bright clusters for  $\sigma_8 = 1.2$ . Also plotted for reference are the expected primary anisotropy and the observed upper limits reported by OVRO (20 GHz) and ATCA (8.7 GHz).